

# Journal of Electronic Imaging

JElectronicImaging.org

## Single underwater image enhancement based on color cast removal and visibility restoration

Chongyi Li  
Jichang Guo  
Bo Wang  
Runmin Cong  
Yan Zhang  
Jian Wang

# Single underwater image enhancement based on color cast removal and visibility restoration

Chongyi Li,<sup>a</sup> Jichang Guo,<sup>a,\*</sup> Bo Wang,<sup>a</sup> Runmin Cong,<sup>a</sup> Yan Zhang,<sup>a,b</sup> and Jian Wang<sup>a,c</sup>

<sup>a</sup>Tianjin University, School of Electronic Information Engineering, No. 92, Weijing Road, Nankai District, Tianjin 300072, China

<sup>b</sup>Tianjin Chengjian University, School of Electronic Information Engineering, No. 26, Jinjing Road, Xiqing District, Tianjin 300384, China

<sup>c</sup>National Ocean Technology Center, No. 60, Xianyang Road, Nankai District, Tianjin 300072, China

**Abstract.** Images taken under underwater condition usually have color cast and serious loss of contrast and visibility. Degraded underwater images are inconvenient for observation and analysis. In order to address these problems, an underwater image-enhancement method is proposed. A simple yet effective underwater image color cast removal algorithm is first presented based on the optimization theory. Then, based on the minimum information loss principle and inherent relationship of medium transmission maps of three color channels in an underwater image, an effective visibility restoration algorithm is proposed to recover visibility, contrast, and natural appearance of degraded underwater images. To evaluate the performance of the proposed method, qualitative comparison, quantitative comparison, and color accuracy test are conducted. Experimental results demonstrate that the proposed method can effectively remove color cast, improve contrast and visibility, and recover natural appearance of degraded underwater images. Additionally, the proposed method is comparable to and even better than several state-of-the-art methods. © 2016 SPIE and IS&T [DOI: [10.1117/1.JEI.25.3.033012](https://doi.org/10.1117/1.JEI.25.3.033012)]

Keywords: underwater image enhancement; color correction; contrast enhancement; visibility restoration.

Paper 16095 received Feb. 5, 2016; accepted for publication May 20, 2016; published online Jun. 9, 2016.

## 1 Introduction

Since the mysterious underwater world contains abundant resources, the research of underwater imaging has drawn much attention recently. However, underwater imaging faces three main problems: color cast (a tint of a particular color, usually unwanted, that affects the whole of a photographic image), degraded contrast and visibility, and blurred features and details due to the physical properties of an underwater medium. As shown in Fig. 1, light intensity decreases with traveling distance in water.<sup>1</sup> In general, blue light travels the longest in water because it has the shortest wavelength, followed by green light and then red light. Thus, underwater images usually tend to appear bluish or greenish. More importantly, the further the objects are laid in an underwater environment, the more serious the color cast will be. As shown in Fig. 2, an underwater image can be represented as a linear superposition of a direct component that reflects light by the objects, a forward-scattering component that randomly deviates light on its way to the camera, and a backscattering component that reflects light toward the camera before the light actually reaches the objects.<sup>2–4</sup> Light absorption degrades the energy of direct light and then causes a hazy image background. Meanwhile, such forward scattering results in blurring of image features, whereas backscattering masks details of the scenario. In addition, macroscopic floating particles bring unwanted noise and increase the effects of absorption and scattering. The limited range of visibility, poor contrast and brightness, and serious color cast of underwater images are caused by the above-mentioned factors. Degraded underwater images show some limitations when being used for observation and analysis,

such as marine biology and archaeology,<sup>5</sup> marine ecological research,<sup>6</sup> aquatic robot inspection,<sup>7</sup> and inspection of columns of offshore platforms.<sup>8</sup> Improving visual quality of degraded underwater images by just using image-processing strategies has been an active research effort in underwater vision and robotics within the last decade.

In this paper, a method for underwater image enhancement is proposed based on color cast removal and visibility restoration. First, a simple yet effective color-correction algorithm is employed to remove color cast of underwater images. Then, a visibility restoration algorithm is proposed to recover the visibility and contrast of underwater images. Qualitative and quantitative comparisons as well as color accuracy tests are conducted to assess the performance of the proposed method. Experiments demonstrate that our results have natural color and appearance, as well as good visibility and contrast. In addition, our method is comparable to and even better than seven state-of-the-art methods.

This paper introduces the following main contributions:

1. A simple yet effective color cast removal algorithm is proposed based on the modification of a previous work. The proposed color cast removal algorithm estimates saturation control parameter by the optimization theory instead of the heuristic values used in previous work. Our color cast removal algorithm has better performance than those used in previous work.
2. A visibility restoration algorithm is proposed. Compared with other visibility restoration algorithms, the proposed algorithm combines the minimum information loss principle with the characteristics of light

\*Address all correspondence to: Jichang Guo, E-mail: [jcguo@tju.edu.cn](mailto:jcguo@tju.edu.cn)

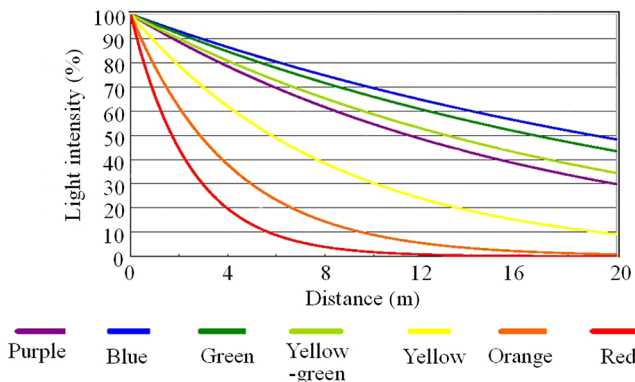


**Fig. 1** Light intensity in water. From left to right: red light, orange light, yellow light, purple light, yellow-green light, green light, and blue light.

traveling in water and restores the three color channels in an underwater image separately.

3. A global background light estimation algorithm is proposed based on the hierarchical searching technique and optical properties. Compared with other background light algorithms, the proposed algorithm can successfully reduce the effects of bright objects and floating particles.

This paper is organized as follows. Existing work related to underwater image enhancement and restoration is described in Sec. 2. The proposed method is introduced in Sec. 3. Different techniques are used to assess and compare experimental results in Sec. 4. This paper is concluded in Sec. 5.

## 2 Related Work

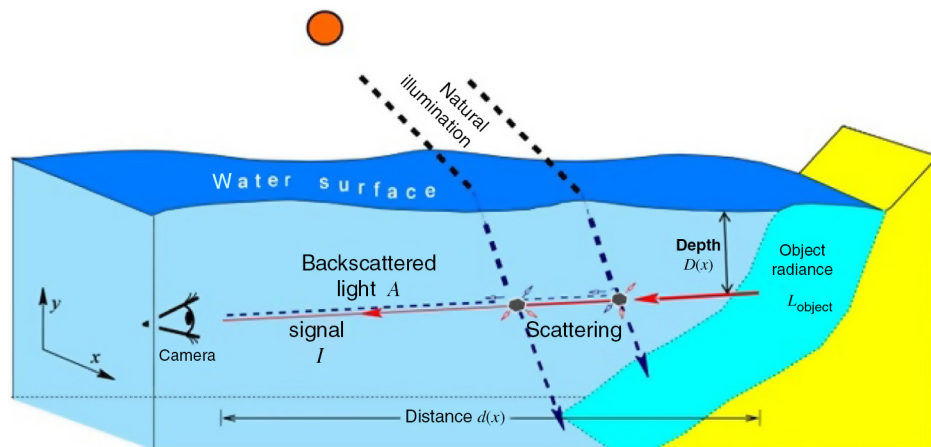
Underwater image-enhancement and restoration techniques have attracted considerable attention in recent years and can be classified into three main categories: single underwater image-enhancement techniques, single underwater image-restoration techniques, and specific techniques.

Single underwater image-enhancement techniques improve contrast and color of underwater images via modifying image pixel values. Iqbal et al.<sup>9</sup> proposed an integrated color model (ICM) to enhance degraded underwater images. ICM method can equalize the contrast of underwater images

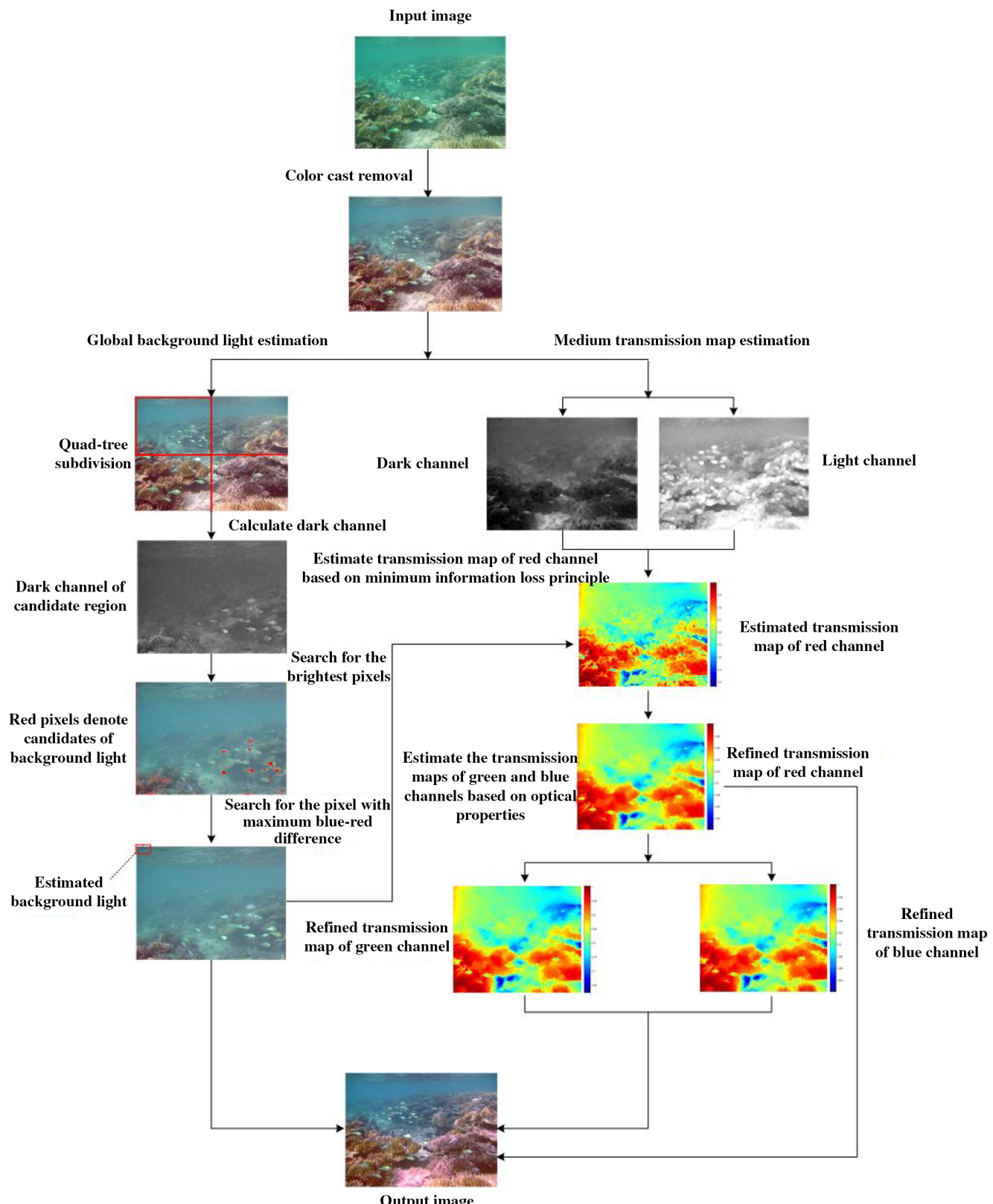
and address the problem of lighting. A few years later, an unsupervised color-correction method was proposed by Iqbal et al.<sup>10</sup> to achieve underwater image enhancement based on color balance and histogram stretching. Ancuti et al.<sup>11</sup> developed a method to enhance the quality of underwater images and videos based on the fusion principle. The enhanced images and videos have better exposure of dark regions and increased global contrast. Fu et al.<sup>12</sup> processed color cast, underexposure, and blurring of underwater imaging using a retinex model and an alternating direction optimization algorithm. Ghani and Isa<sup>13,14</sup> modified and extended the ICM method for reducing underenhanced and overenhanced areas.

Single underwater image-restoration techniques restore degraded underwater images using a physical model of underwater imaging. The purpose of restoration is to estimate the parameters of the physical model and then restore underwater images by reverse compensation processing. Carlevaris-Bianco et al.<sup>15</sup> estimated the depths of an imaging scene by exploiting the difference in attenuation among three color channels of an underwater image. The effects of light scattering in underwater images can be removed. Chiang and Chen<sup>16</sup> restored underwater images by combining a dehazing algorithm<sup>17</sup> with the wavelength compensation algorithm. As a result, the effects of haze from scattering and the distortion from color cast can be reduced. Wen et al.<sup>18</sup> developed an underwater imaging model by exploring the difference of light attenuation in between atmosphere and water. Serikawa and Lu<sup>19</sup> addressed the problems of scattering and color cast for underwater images by compensating the attenuation discrepancy along the propagation path. Galdran et al.<sup>20</sup> proposed a red channel method, where color associated with short wavelength is recovered, which leads to a restoration of lost contrast. Zhao et al.<sup>21</sup> obtained the inherent optical properties of water from background color. Li and Guo<sup>22</sup> proposed an underwater image-enhancement method based on a dehazing algorithm and a filtering algorithm. Lu et al.<sup>23</sup> restored underwater images through compensating the attenuation discrepancy along the propagation path.

There are several specific techniques for improving the quality of underwater images. Schechner and Karpel<sup>4,24</sup> restored visibility of underwater images based on a couple of images taken through a polarizer at different



**Fig. 2** Schematic of underwater optical imaging.

**Fig. 3** Flowchart of the proposed method.

orientations. Ouyang et al.<sup>25</sup> enhanced underwater images by an underwater laser line scan system. To obtain clear images in turbid water, He and Seet<sup>26</sup> developed a divergent-beam lidar imaging system.

However, some results of single underwater image-enhancement methods are overenhanced or underenhanced since those methods fail to consider the physical model of underwater imaging. Some assumptions made in single

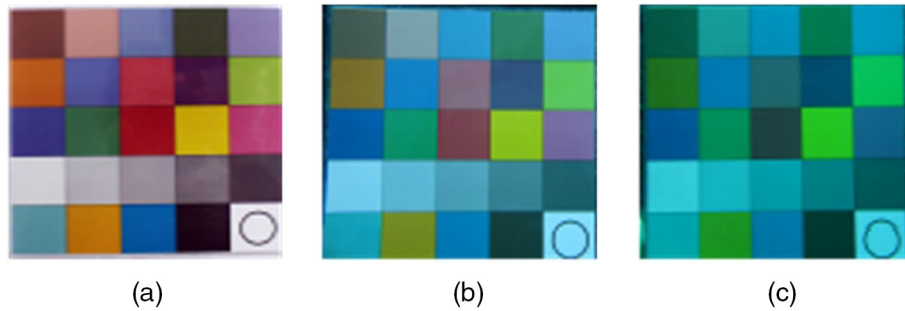


**Fig. 4** An example of underwater image color cast: (a) standard Color-Checker Chart image taken in air; (b) Color-Checker Chart image taken at the depth of 5 m in water; and (c) Color-Checker Chart image taken at the depth of 10 m in water.

underwater image-restoration methods are not suitable for many situations. Despite the effectiveness of specific techniques, these techniques show some problems that potentially reduce their practical applicability. For instance, hardware devices employed in the specific techniques may be relatively expensive. Therefore, an effective underwater image-enhancement method that employs image-processing strategy is desired.

---

**Algorithm 1** Optimize the saturation control parameter.

---

**Input:** The standard color-checker image  $f(x)_{\text{STD}}^c$  and the color-checker images taken at different depths  $f(x)^c$

**Initialization:** MIN =  $+\infty$

**for**  $\mu^r = 0.5:0.5:10$

**for**  $\mu^g = 0.5:0.5:10$

**for**  $\mu^b = 0.5:0.5:10$

$$f(x)_{\text{CR}}^c = \frac{f(x)^c - C(x)_{\min}^c}{C_{\max}^c - C(x)_{\min}^c} \times 255 \leftarrow \text{color-corrected color-checker image}$$

$$= \frac{f(x)^c - f(x)_{\text{mean}}^c + \mu^c \cdot f(x)_{\text{var}}^c}{2\mu^c \cdot f(x)_{\text{var}}^c} \times 255$$

$$E = \sum \|f(x)_{\text{CR}}^c - f(x)_{\text{STD}}^c\|^2 \leftarrow \text{cost function}$$

**if**  $E \leq \text{MIN}$

$$E = \text{MIN}$$

$$\mu_{\text{out}}^r = \mu^r$$

$$\mu_{\text{out}}^g = \mu^g$$

$$\mu_{\text{out}}^b = \mu^b$$

**end**

**end**

**end**

**Output:** Optimized saturation control parameter

---

### 3 Proposed Method

The proposed method consists of two main parts: color cast removal and visibility restoration. A flowchart of the proposed method is shown in Fig. 3.

As shown in Fig. 3, input underwater image is first processed by our modified color cast removal algorithm. The proposed color cast removal algorithm is presented in Sec. 3.2. After that, global background light is estimated by combining the hierarchical searching technique with optical properties. The proposed global background light estimation algorithm is introduced in Sec. 3.3.1. Finally, the medium transmission maps of three color channels in an underwater image are estimated separately. The medium transmission map of red color channel is estimated based on the minimum information loss principle. Then, the estimated medium transmission map of red color channel is refined by guided filter in order to reduce the effects of blocking artifacts. The proposed medium transmission map estimation algorithm of red color channel is given in Sec. 3.3.2. The medium transmission maps of green and blue color channels are estimated based on the refined medium transmission map of red color channel and the characteristics of light traveling in water. The proposed algorithm for estimating medium transmission maps of green and blue color channels is presented in Sec. 3.3.3. At last, the clear underwater image is obtained according to the underwater imaging model.

#### 3.1 Relation to Prior Work

Compared with the color-correction algorithm proposed by Fu et al.,<sup>12</sup> our color cast removal algorithm is based on the modification of their work. In Fu et al.'s work, a parameter that controls the saturation of color-corrected underwater image is selected through subjective experiments. To more accurately estimate this parameter, the least squares optimization theory is employed in our color cast removal algorithm. The details are presented in Sec. 3.2. Unlike previous underwater image visibility restoration methods that apply original dark channel prior algorithm to restore three color channels with the same equation (i.e., Carlevaris-Bianco et al.'s method<sup>15</sup>), compensate the attenuation discrepancy along the propagation path (i.e., Chiang and Chen's method,<sup>16</sup> Serikawa and Lu's method<sup>19</sup>), or propose a new underwater imaging model (i.e., Wen et al.'s method<sup>18</sup>), our visibility restoration algorithm is based on the minimum information loss principle and the characteristics of light traveling in water and processes three color channels separately. The details are presented in Sec. 3.3.

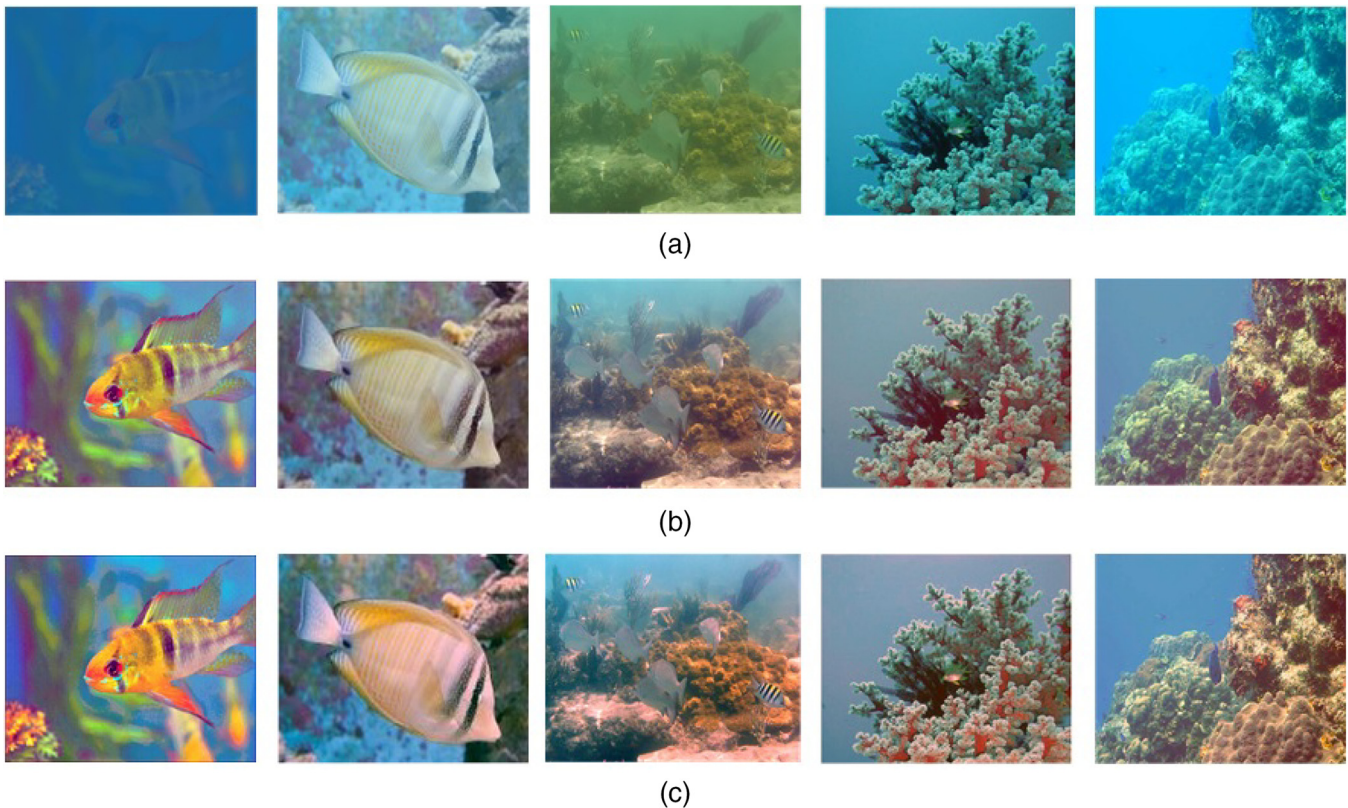


**Fig. 5** Color-corrected results comparison: (a) raw underwater images; (b) Fu et al.'s results ( $\mu' = \mu^g = \mu^b = 3$ ); and (c) our color cast removal algorithm's results ( $\mu' = 2$ ,  $\mu^g = 3.25$ ,  $\mu^b = 2.5$ ).

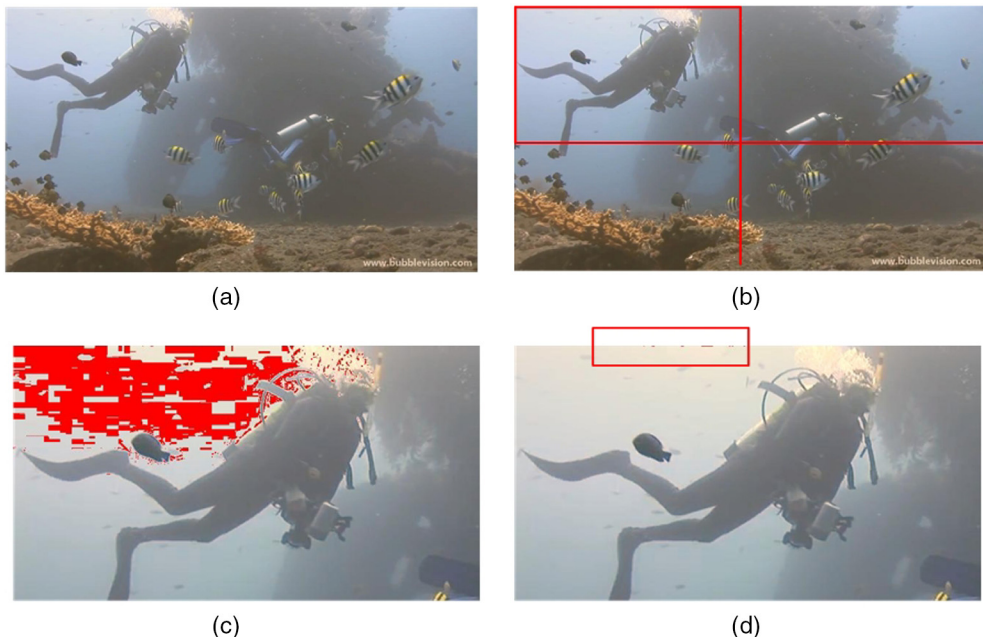


**Fig. 6** An example to illustrate the global background light estimation algorithm: (a) color-corrected underwater image; (b) result of the quad-tree subdivision, where red rectangle represents the candidate region; (c) result of searching for the brightest pixels in the dark channel, where red pixels are the brightest pixels in the dark channel; and (d) result of searching for the pixels with the maximum blue-red difference, where red pixels in the red rectangle are the candidates of global background light.

### 3.2 Color Cast Removal

Underwater images tend to appear bluish or greenish color cast because blue light travels the longest in water, followed

by green light, and then red light. Figure 4 shows an example of underwater image color cast.

As shown in Fig. 4, compared with the standard Color-Checker Chart image, some colors of underwater Color-

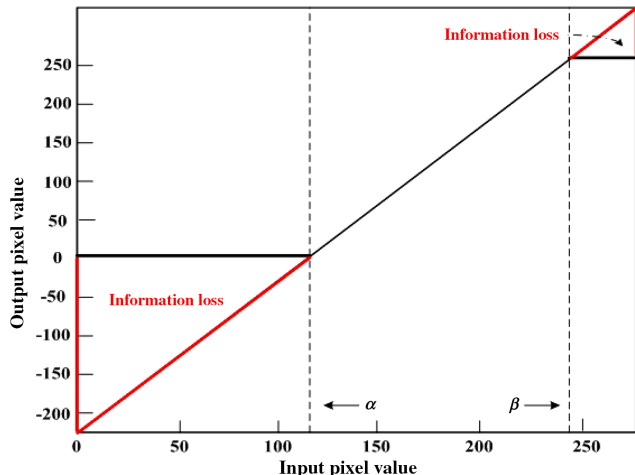


**Fig. 7** An example of the medium transformation map function: input pixel values are mapped to output pixel values, depicted by the black line. The red regions denote the information loss due to the truncation of output pixel values.

Checker Chart images disappear and change. The purpose of our color cast removal algorithm is to restore relatively genuine color of underwater images. Experiments found that numerous successful solutions that can solve the problem of color cast for common images perform poorly for underwater images. In order to remove color deviation in underwater images, we modified a simple color correction algorithm,<sup>12</sup> which demonstrated that color cast of underwater images can be corrected using a maximum and minimum color deviation stretching algorithm. The details are introduced as follows.

The mean values and mean square error (MSE) values of each color channel are calculated. Then, the maximum and the minimum color deviation in each color channel are defined as

$$\begin{cases} f(x)_\text{max}^c = f(x)_\text{mean}^c + \mu^c \cdot f(x)_\text{var}^c, \\ f(x)_\text{min}^c = f(x)_\text{mean}^c - \mu^c \cdot f(x)_\text{var}^c, \end{cases} \quad c \in \{r, g, b\}, \quad (1)$$

where  $f(x)_\text{mean}^c$  is the mean value,  $f(x)_\text{var}^c$  is the MSE value, and  $\mu^c$  is a parameter to control the saturation of the color-corrected underwater image. Color-corrected underwater

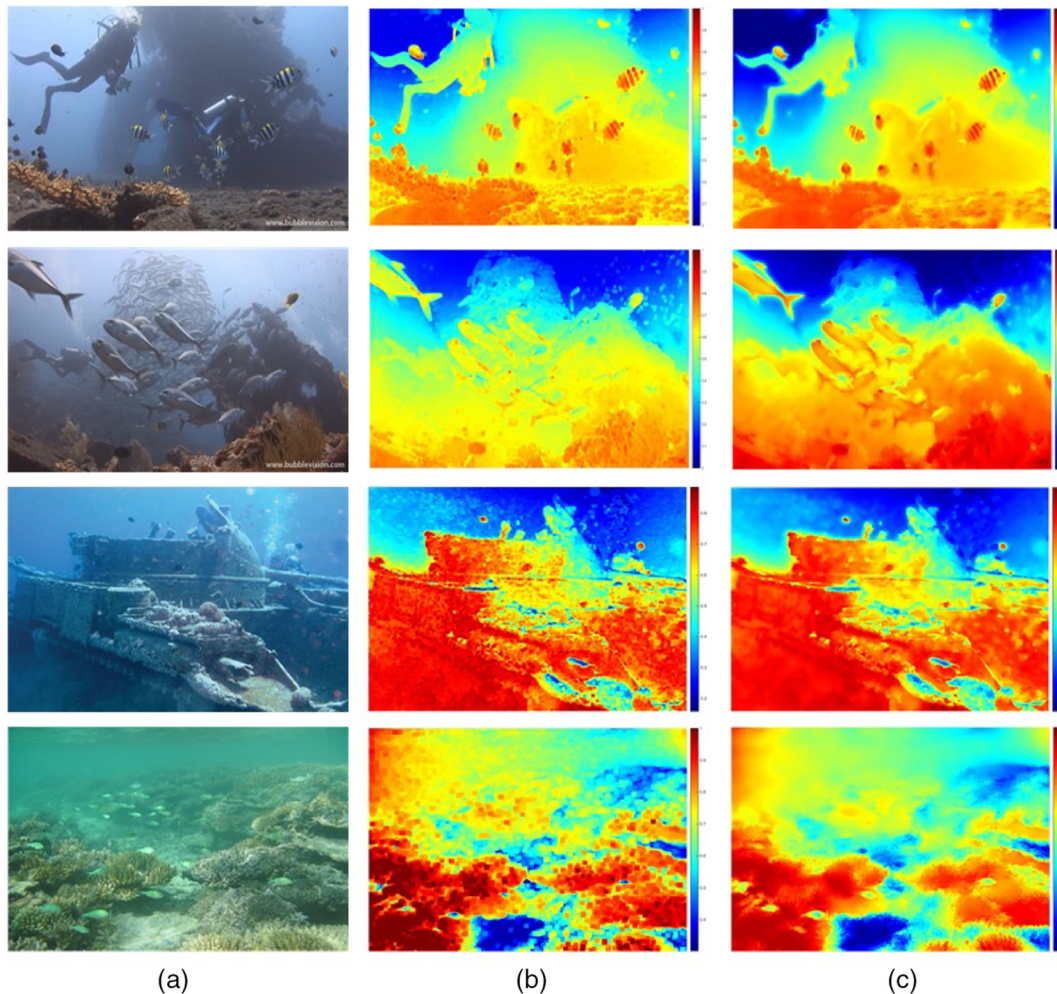


**Fig. 8** The medium transmission maps of red channel: (a) raw underwater images; (b) coarse medium transmission maps; and (c) refined medium transmission maps. In the medium transmission maps, the color bar represents the different pixel values.

image  $f(x)_{\text{CR}}^c$  can be obtained using a maximum and minimum color deviation stretching algorithm.

$$\begin{aligned} f(x)_{\text{CR}}^c &= \frac{f(c)^c - f(x)_{\min}^c}{f(c)_{\max}^c - f(x)_{\min}^c} \times 255 \\ &= \frac{f(c)^c - f(x)_{\text{mean}}^c + \mu^c \cdot f(x)_{\text{var}}^c}{2\mu^c \cdot f(x)_{\text{var}}^c} \times 255, \end{aligned} \quad (2)$$

where  $f(x)$  is input image. In Fu et al.'s method,<sup>12</sup> the saturation control parameter  $\mu^c$  is set to 3 for three color channels based on subjective visual inspection. To more accurately remove color cast, the least squares optimization theory is employed to estimate the optimized saturation control parameter in this paper. The saturation control parameter  $\mu^c$  is approximately estimated by minimizing the least squares between the standard Color-Checker Chart image [Fig. 4(a)] and the corrected versions of underwater Color-Checker Chart images [Figs. 4(b) and 4(c)]. Removing color

cast of underwater images captured in turbid water is not discussed in this paper.

First, a cost function  $E$  that represents the difference of image intensity between the corrected version of the underwater Color-Checker Chart image and the standard Color-Checker Chart image is defined as

$$E = \sum \|f(x)_{\text{CR}}^c - f(x)_{\text{STD}}^c\|^2, \quad c \in \{r, g, b\}, \quad (3)$$

where  $f(x)_{\text{CR}}^c$  represents the color-corrected version of the underwater Color-Checker Chart image and  $f(x)_{\text{STD}}^c$  is the standard Color-Checker Chart image.

Next, the unknown saturation control parameter  $\mu^c$  that best minimizes the cost function  $E$  needs to be estimated. For simplification, we solve this problem by iteration strategy. The range of  $\mu^c$  is from 0.5 to 10. The step of iteration is set to 0.5. The optimization algorithm is outlined in Algorithm 1.

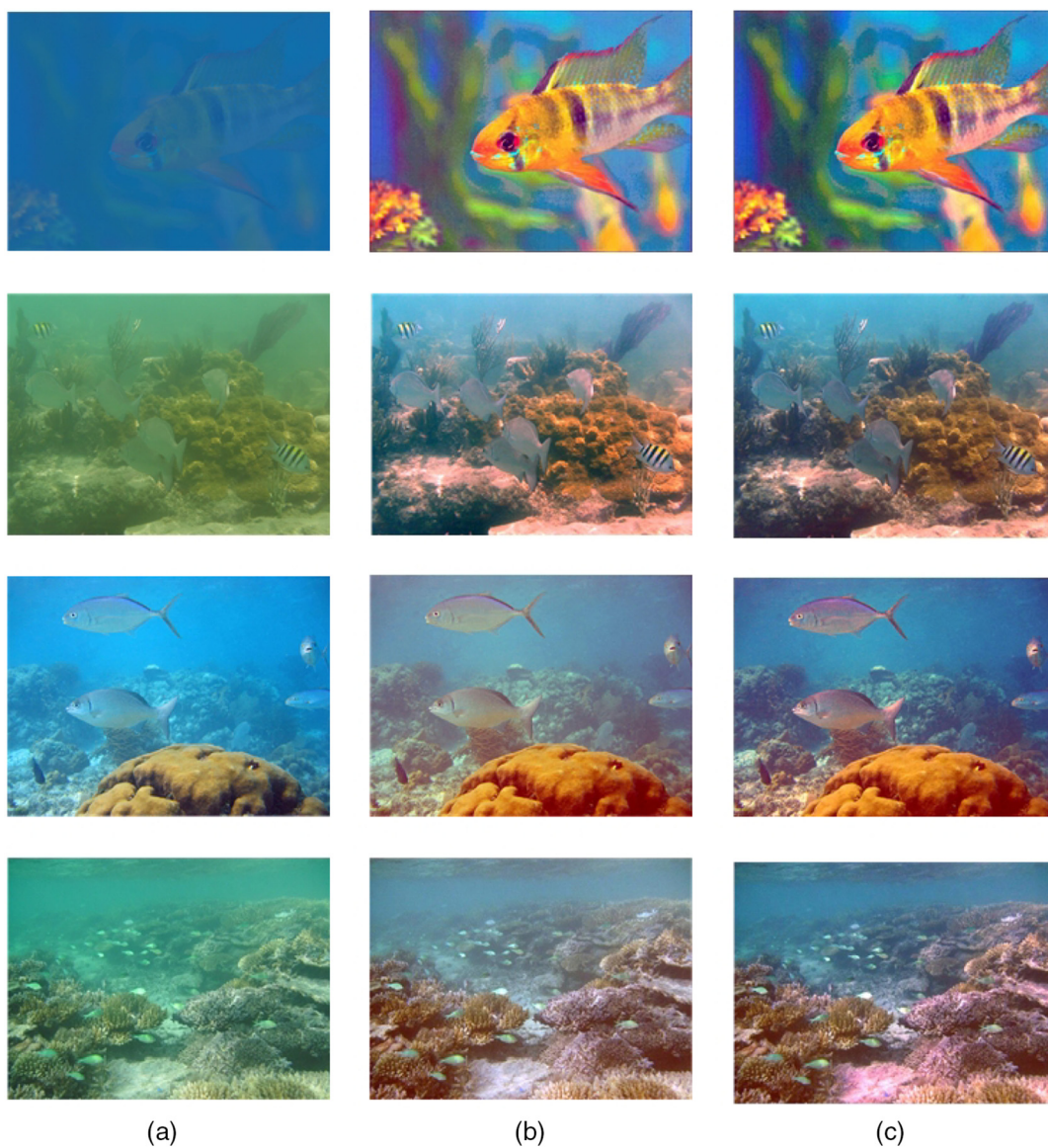


**Fig. 9** Some results of the proposed method: (a) raw underwater images; (b) results of our color cast removal algorithm; and (c) results of our visibility restoration algorithm.

For the color-corrected underwater Color-Checker Chart image captured at 5 m,  $\mu^r = 2.5$ ,  $\mu^g = 3.5$ , and  $\mu^b = 2.5$  make the cost function minimum. Meanwhile,  $\mu^r = 1.5$ ,  $\mu^g = 3$ , and  $\mu^b = 2.5$  make the cost function minimum for the color-corrected underwater Color-Checker Chart image captured at 10 m. To robustly remove color cast of underwater images captured at different depths, the average values of estimated saturation control parameter are used in this paper. The compared results between our color cast removal algorithm and Fu et al.'s color correction algorithm are shown in Fig. 5.

As shown in Fig. 5, compared with Fu et al.'s algorithm, which estimates the saturation control parameter by subjective experiments, our color cast removal algorithm can unveil more color details and improve the brightness of underwater images. Further comparison can be seen in Sec. 4.3.

### 3.3 Visibility Restoration

Following previous work,<sup>15,20</sup> the simplified underwater imaging model can be described as

$$I^c(x) = J^c(x)t^c(x) + B^c[1 - t^c(x)], \quad c \in \{r, g, b\}, \quad (4)$$

where  $I(x)$  is the degraded image,  $J(x)$  is the clear image,  $B$  is the global background light, and  $t(x) \in [0, 1]$  is the medium transmission map. The purpose of visibility

restoration is to restore  $J(x)$  from  $I(x)$ . To solve this ill-posed problem, the proposed visibility restoration algorithm includes three main processing steps: global background light estimation, medium transmission map of red channel estimation, and medium transmission maps of green and blue channels estimation.

#### 3.3.1 Global background light estimation

To estimate the global background light, we first use a quad-tree subdivision technique,<sup>27–29</sup> then remove bright objects through the dark channel prior algorithm,<sup>17</sup> and finally determine the global background light according to optical properties. The global background light estimation algorithm is shown step by step in Fig. 6.

First, a color-corrected underwater image is divided into four rectangular regions. The score of each region is defined as the average pixel value subtracted by the standard deviation of the pixel values within the region. The region with the highest score is defined as the candidate region. Then, according to the conclusion of the dark channel prior algorithm, 0.1% of the brightest pixels in the dark channel of the candidate region are picked up for avoiding the effects of suspended particles and foreground objects. At last, one pixel with the maximum blue-red difference among the brightest pixels is selected as the estimated global background light. According to optical properties of underwater

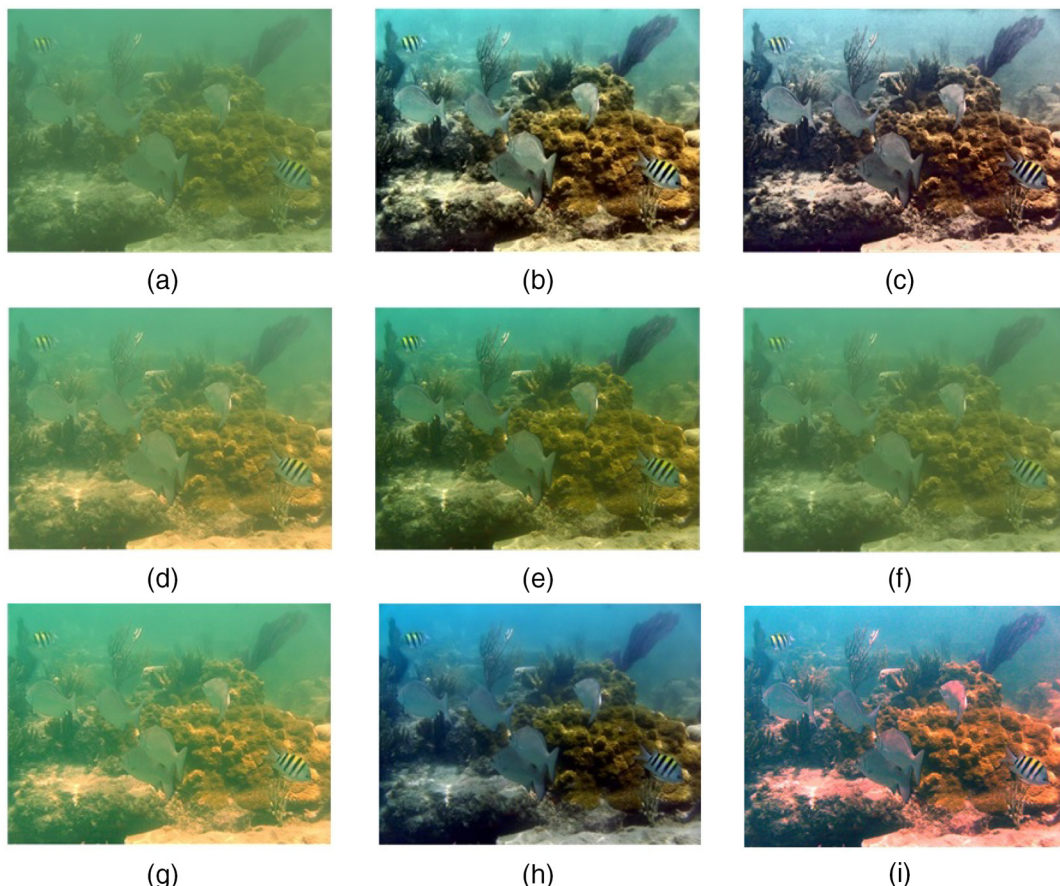


**Fig. 10** Qualitative comparison on image Fish: (a) raw underwater image with size 512 × 384; (b) method of Ancuti et al.; (c) method of Fu et al.; (d) method of Chiang and Chen; (e) method of He et al.; (f) method of Carlevaris-Bianco et al.; (g) method of Serikawa and Lu; (h) method of Galdran et al.; and (i) our method.

imaging, blue light travels the longest in water, followed by green light and then red light. In this way, the effects caused by the objects that are brighter than the global background light can be removed. Consequently, the selection of the pixel with the maximum blue-red difference guarantees the robustness of the proposed global background light estimation algorithm.

### 3.3.2 Medium transmission map of red channel estimation

Next, visibility restoration depends on the selection of medium transmission map  $t^c$ . Equation (4) can be rewritten as a medium transmission map function.

$$J^c(x) = \frac{1}{t^c(x)} [I^c(x) - B^c] + B^c. \quad (5)$$

The medium transmission map function in Eq. (5) is shown in Fig. 7.

As shown in Fig. 7, the medium transformation map function maps an input pixel value  $I^c(x)$  to an output value  $J^c(x)$ . Note that input values in  $[\alpha, \beta]$  are mapped to output values in the full dynamic range  $[0, 255]$ , where the medium transmission map  $t^c$  determines the valid input range  $[\alpha, \beta]$ . If some input values lie outside the valid input range, the mapped output values do not belong to the valid output range

$[0, 255]$ . In such a situation, saturation of pixel colors occurs in some pixel values, which are truncated to 0 or 255. The truncated pixel values mean information loss and can be seen in the red regions in Fig. 7.

To reduce the information loss, an optimal medium transmission map should be selected. Assuming that the medium transmission map in the local block has the same pixel value, we first define the information loss cost  $\text{Infor}_{\text{loss}}$  in a local block  $D$  for red channel as

$$\begin{aligned} \text{Infor}_{\text{loss}} = & \sum_{x \in D} (\{\min[0, J^r(x)]\}^2 \\ & + \{\max[0, J^r(x) - 255]\}^2). \end{aligned} \quad (6)$$

Combining with Eq. (5), Eq. (6) can be rewritten as

$$\begin{aligned} \text{Infor}_{\text{loss}} = & \sum_{x \in D} \left( \left\{ \min \left[ 0, \frac{I^r(x) - B^r}{t^r} + B^r \right] \right\}^2 \right. \\ & \left. + \left\{ \max \left[ 0, \frac{I^r(x) - B^r}{t^r} + B^r - 255 \right] \right\}^2 \right). \end{aligned} \quad (7)$$

To minimize information loss, Eq. (7) should satisfy the constraint as follows:

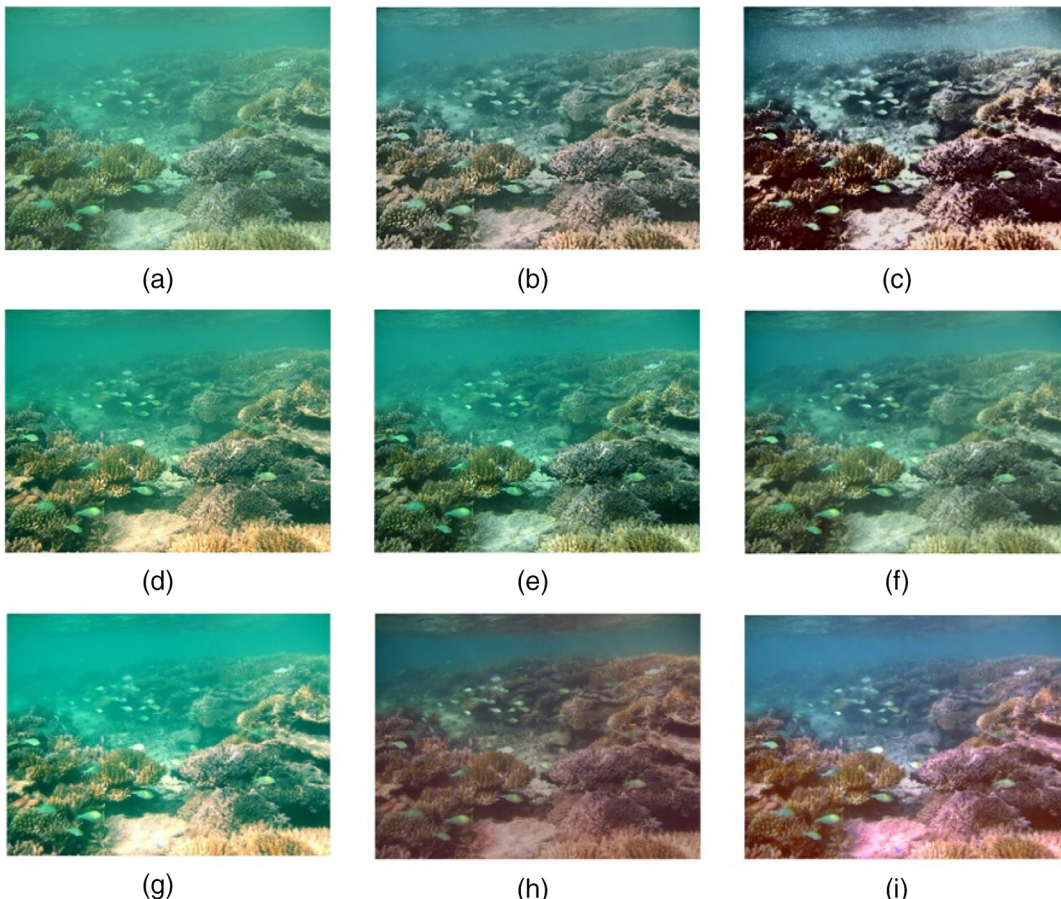


**Fig. 11** Qualitative comparison on image Coral: (a) raw underwater image with size  $512 \times 384$ ; (b) method of Ancuti et al.; (c) method of Fu et al.; (d) method of Chiang and Chen; (e) method of He et al.; (f) method of Carlevaris-Bianco et al.; (g) method of Serikawa and Lu; (h) method of Galdran et al.; and (i) our method.

$$\begin{cases} \min_{x \in D} \left[ \frac{I^r(x) - B^r}{t^r} + B^r \right] \geq 0 \\ \max_{x \in D} \left[ \frac{I^r(x) - B^r}{t^r} + B^r - 255 \right] \leq 0 \end{cases}. \quad (8)$$

Thus, the estimated medium transmission map  $t^{r*}$  can be rewritten as

$$t^{r*} \geq \max \left\{ \min_{x \in D} \left[ \frac{I^r(x) - B^r}{-B^r} \right], \max_{x \in D} \left[ \frac{I^r(x) - B^r}{255 - B^r} \right] \right\}. \quad (9)$$

We select the minimum value that satisfies the constraint in Eq. (9). The guided filter<sup>30</sup> is used to remove the blocking artifacts of the coarse medium transmission map. Some estimated medium transmission maps are shown in Fig. 8.

As shown in Fig. 8, the blocking artifacts are reduced by guided filter. Moreover, the different colors in the medium transmission maps indicate that the medium transmission maps are relatively accurately estimated.

### 3.3.3 Medium transmission maps of green and blue channels estimation

To restore degraded underwater image, the medium transmission maps of green and blue channels are also needed. Since estimating the medium transmission maps of green

and blue channels by the same constraint ignores the correlation of three color channels, the relationship of the medium transmission maps of three color channels is built through exploring the characteristics of light traveling in water.

According to the Lambert–Beer empirical law,<sup>31</sup> the medium transmission map  $t^c$  is determined by the distance  $d(x)$  between the scene point and the camera. The medium transmission map can be expressed as

$$t^c(x) = \exp[-p^c d(x)], \quad c \in \{r, g, b\}, \quad (10)$$

where  $p^c$  is the total attenuation coefficient. However, it is very hard to estimate the total attenuation coefficient due to the complicated underwater imaging situations. Inspired by Ref. 16, the medium transmission map can be rewritten as

$$t^c(x) = \text{Nrer}(\lambda)^{d(x)}, \quad (11)$$

where  $\text{Nrer}(\lambda)$  denotes the normalized residual energy ratio, which depends on the light wavelengths.<sup>32</sup> Based on the estimated medium transmission map of red channel, the distance  $d(x)$  between the scene point and the camera can be estimated as

$$d(x) = \frac{\ln[t^r(x)]}{\ln[\text{Nrer}(r)]}, \quad (12)$$

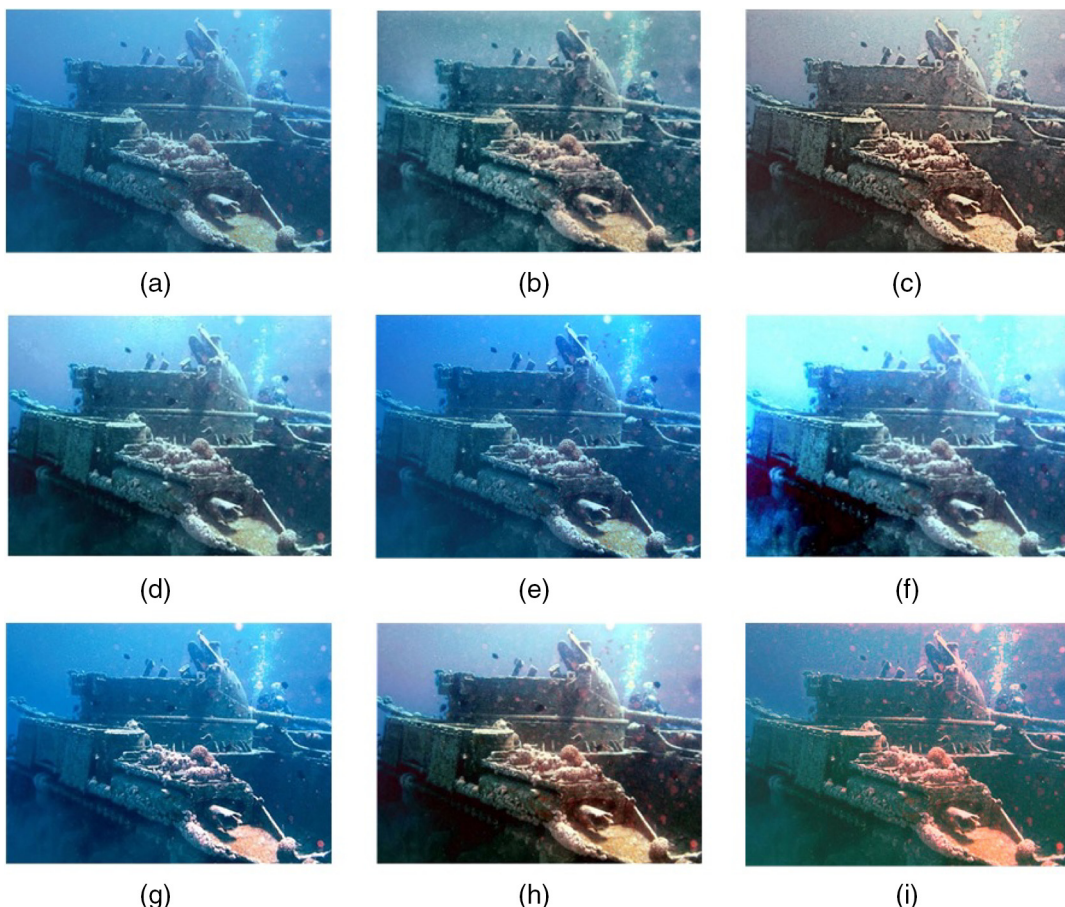


**Fig. 12** Qualitative comparison on image Wreckage: (a) raw underwater image with size  $512 \times 384$ ; (b) method of Ancuti et al.; (c) method of Fu et al.; (d) method of Chiang and Chen; (e) method of He et al.; (f) method of Carlevaris-Bianco et al.; (g) method of Serikawa and Lu; (h) method of Galdran et al.; and (i) our method.

where  $t^r(x)$  is the medium transmission map of the red channel, and  $\text{Nrer}(r)$  represents the normalized residual energy ratio of red channel. In general, for every meter that a light beam passes through, the normalized residual energy ratio  $\text{Nrer}(\lambda)$  can be expressed as follows:

$$\text{Nrer}(\lambda) = \begin{cases} 0.8 \text{ to } 0.85, & \text{if } \lambda = 650 \text{ to } 750 \mu\text{m}, \quad r \text{ (red),} \\ 0.93 \text{ to } 0.97, & \text{if } \lambda = 490 \text{ to } 550 \mu\text{m}, \quad g \text{ (green),} \\ 0.95 \text{ to } 0.99, & \text{if } \lambda = 400 \text{ to } 490 \mu\text{m}, \quad b \text{ (blue).} \end{cases} \quad (13)$$

Consequently, the medium transmission maps of green and blue channels can be estimated as

$$t^g(x) = \text{Nrer}(g)^{d(x)} = \text{Nrer}(g)^{\ln[t^r(x)]/\ln[\text{Nrer}(r)]}, \quad (14)$$

$$t^b(x) = \text{Nrer}(b)^{d(x)} = \text{Nrer}(b)^{\ln[t^r(x)]/\ln[\text{Nrer}(r)]}. \quad (15)$$

In this paper,  $\text{Nrer}(\lambda)$  used for red, green, and blue lights are 83%, 93%, and 97%, respectively. After estimating the global background light and medium transmission maps of three color channels, the restored underwater image can be obtained using Eq. (5). Some results produced by our proposed color cast removal algorithm and visibility restoration algorithm are shown in Fig. 9.

As shown in Fig. 9, our color cast removal algorithm can successfully remove color deviation of the raw underwater images. Our visibility restoration algorithm can improve the contrast, brightness, and details, especially for the background of the raw underwater images.

## 4 Experimental Results

Unlike the common image-quality assessment or common image-restoration areas, there is no easy way to have a reference image, which makes underwater image-enhancement and restoration methods difficult to be assessed. In order to evaluate the performance of the proposed method, qualitative comparison, quantitative comparison, and a color accuracy test are carried out. The state-of-the-art methods used for comparisons include the methods of Ancuti et al.,<sup>11</sup> Fu et al.,<sup>12</sup> Chiang and Chen,<sup>16</sup> He et al.,<sup>17</sup> Carlevaris-Bianco et al.,<sup>15</sup> Serikawa and Lu,<sup>19</sup> and Galdran et al.<sup>20</sup> The methods of Ancuti et al.<sup>11</sup> and Fu et al.<sup>12</sup> are representative enhancement methods for underwater images. The methods of Chiang and Chen,<sup>16</sup> He et al.,<sup>17</sup> Carlevaris-Bianco et al.,<sup>15</sup> Serikawa and Lu,<sup>19</sup> and Galdran et al.<sup>20</sup> are classical restoration methods based on an imaging physical model. Our method is compared with these representative enhancement methods (i.e., Ancuti et al.<sup>11</sup> and Fu et al.<sup>12</sup>) because our method is a type of enhancement method. In addition, our method is based on an underwater imaging physical model. Therefore, our method is also compared with some physics-based restoration

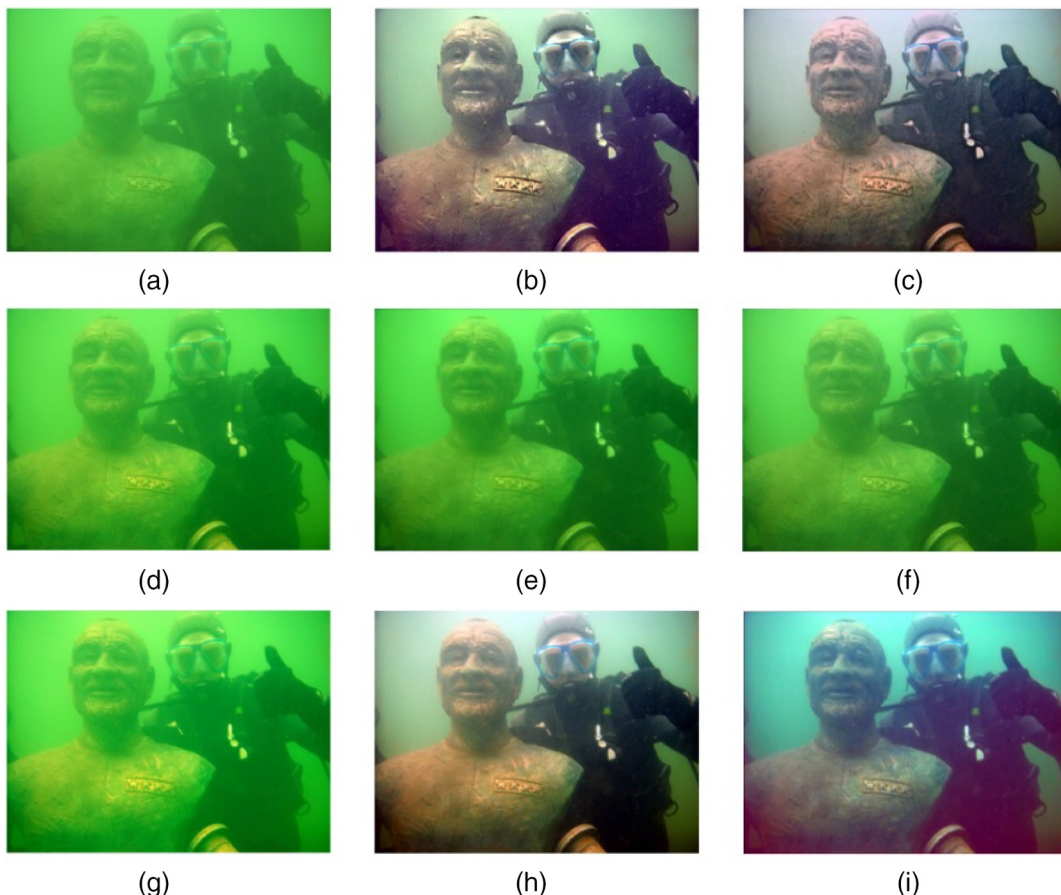


**Fig. 13** Qualitative comparison on image Diver 1: (a) raw underwater image with size  $512 \times 384$ ; (b) method of Ancuti et al.; (c) method of Fu et al.; (d) method of Chiang and Chen; (e) method of He et al.; (f) method of Carlevaris-Bianco et al.; (g) method of Serikawa and Lu; (h) method of Galdran et al.; and (i) our method.

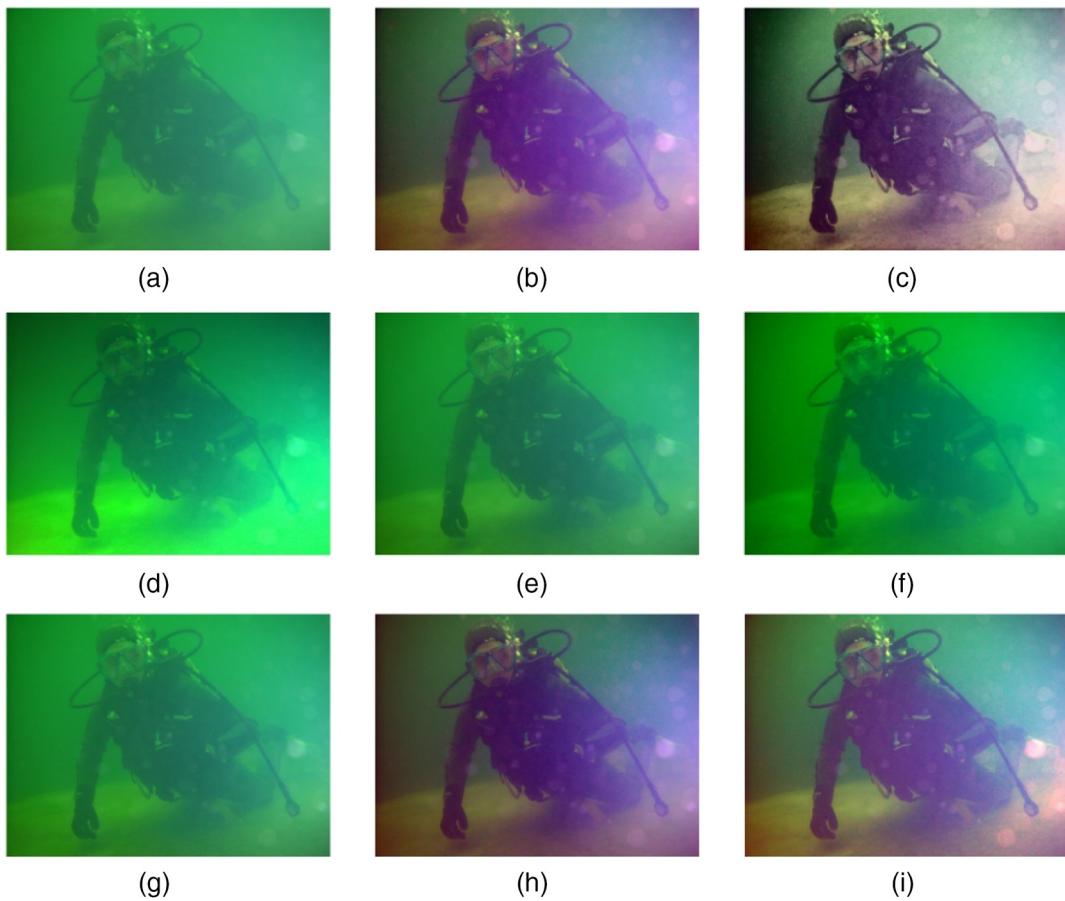


**Fig. 14** Qualitative comparison on image Diver 2: (a) raw underwater image with size  $512 \times 384$ ; (b) method of Ancuti et al.; (c) method of Fu et al.; (d) method of Chiang and Chen; (e) method of He et al.; (f) method of Carlevaris-Bianco et al.; (g) method of Serikawa and Lu; (h) method of Galdran et al.; and (i) our method.

methods (i.e., Chiang and Chen,<sup>16</sup> He et al.,<sup>17</sup> Carlevaris-Bianco et al.,<sup>15</sup> Serikawa and Lu,<sup>19</sup> and Galdran et al.<sup>20</sup>).

#### 4.1 Qualitative Comparison

As shown in Figs. 10–14, our results are compared with those of the above-mentioned state-of-the-art methods using qualitative comparison.

As shown in Figs. 10–14, our method can successfully remove color cast and restore visibility of degraded underwater images. Our results are characterized by improved contrast and brightness, relatively genuine color, good visibility, and natural appearance. The methods of Ancuti et al. and Fu et al. can increase contrast and unveil details of raw underwater images. However, there are overenhanced and

**Table 1** Average values in terms of ENTROPY, PCQI, UCIQE, and VER.

Image	Method	ENTROPY	PCQI	UCIQE	VER
Figs. 10–14	Ancuti et al.	7.7726	0.8142	0.5322	3.4218
	Fu et al.	7.6414	1.1552	0.4850	<b>4.1459</b>
	Chiang and Chen	6.8570	0.3216	0.4047	-0.4863
	He et al.	6.7139	1.1203	0.4525	2.7620
	Carlevaris-Bianco et al.	6.5466	0.4241	0.4451	-0.3601
	Serikawa and Lu	6.7426	0.4587	0.4274	0.0372
	Galdran et al.	7.7558	0.4088	<b>0.6671</b>	2.1521
	Our	<b>7.8129</b>	<b>1.1563</b>	0.5413	3.4721

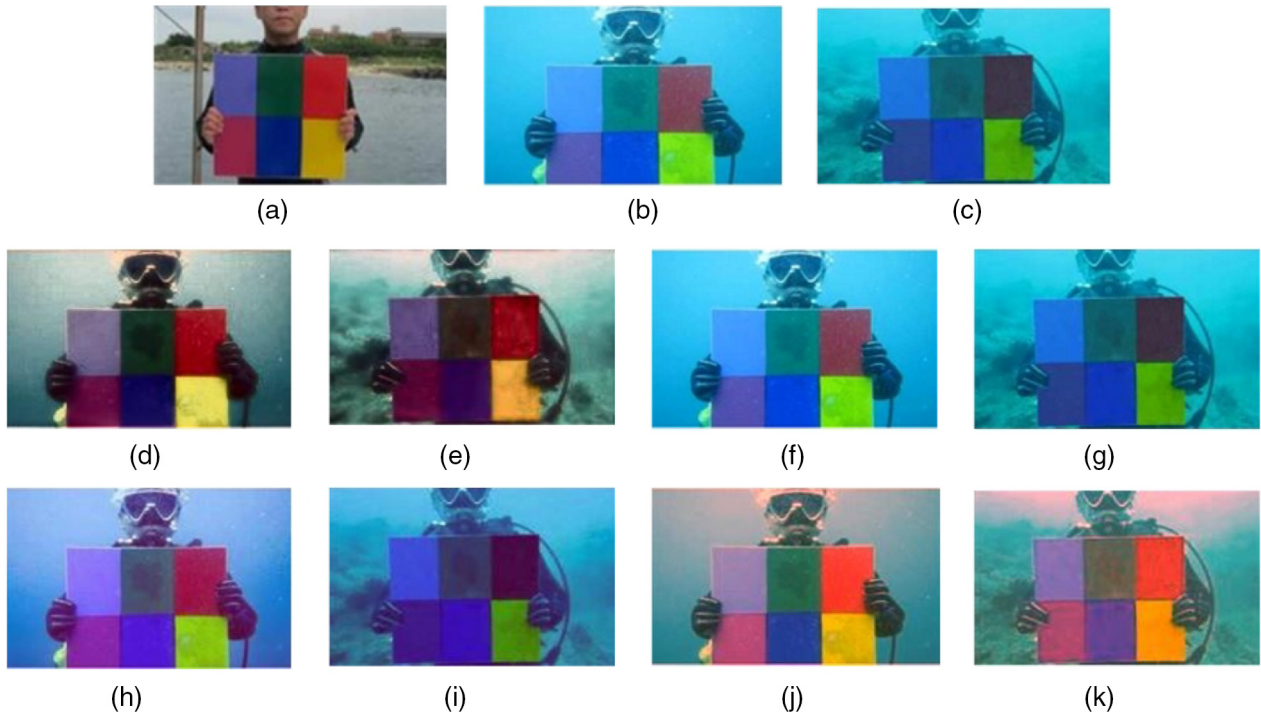


**Fig. 15** Color accuracy test: (a) standard Color-Checker Chart image with size  $256 \times 187$ ; (b) Color-Checker Chart image taken at the depth of 5 m; (c) Color-Checker Chart image taken at the depth of 15 m; (d) result of (b) using the method of Fu et al.; (e) result of (c) using the method of Fu et al.; (f) result of (b) using the method of He et al.; (g) result of (c) using the method of He et al.; (h) result of (b) using the method of Galdran et al.; (i) result of (c) using the method of Galdran et al.; (j) result of (b) using our method; and (k) result of (c) using our method.

underenhanced areas (i.e., the medal in Fig. 13 is overenhanced) in the results of Ancuti et al. and Fu et al. due to ignoring the physical model of underwater optical imaging. Moreover, the appearance of the enhanced images in the methods of Ancuti et al. and Fu et al. is not as natural as in our results. The methods of Chiang and Chen, He et al., Carlevaris-Bianco et al., and Serikawa and Lu can improve the visual quality of raw underwater images. However, color and details in the enhanced results are not good enough. The method of Galdran et al. can effectively restore the visibility and relatively genuine color of degraded underwater images. In contrast, the details and brightness of the enhanced results are not as good as in our results. Therefore, the qualitative comparison demonstrates that our results are the most visually appealing in the compared results.

#### 4.2 Quantitative Comparison

Following the previous work, entropy (ENTROPY), which represents the contained information, patch-based contrast quality index (PCQI), which indicates the change of contrast,<sup>33</sup> underwater color image-quality evaluation (UCIQE), which represents the balance of chroma, saturation, and contrast,<sup>34</sup> and visible edges ratio (VER), which represents the ratio of recovered visible edges and visible edges of original image,<sup>35</sup> are used to verify the performance of the proposed method. In the research of underwater image enhancement and restoration, those evaluation metrics are widely employed to assess the performance of different methods.

Table 1 shows the average values in terms of ENTROPY, PCQI, UCIQE, and VER for the five images shown in Figs. 10–14. The values in bold represent the best results.

As shown in Table 1, our method outperforms the other methods in terms of ENTROPY and PCQI values, which demonstrates that our method can effectively increase the information, contrast, and visibility of the raw underwater images. Moreover, our method ranks second in terms of UCIQE and VER values, which indicates that our method can restore the edge information of degraded underwater images and can also well balance chroma, saturation, and contrast of the enhanced underwater images.

#### 4.3 Color Accuracy Test

To verify the color accuracy of our method, two Color-Checker Chart images with six color patches<sup>16</sup> taken at the depths of 5 and 15 m in water are employed. For the limited space, our results are compared with those of several above-mentioned methods (i.e., Fu et al.,<sup>12</sup> He et al.,<sup>17</sup> and Galdran et al.<sup>20</sup>). Additionally, the results of different methods are evaluated by MSE, peak signal-to-noise ratio (PSNR), ENTROPY, PCQI, UCIQE, and VER. The MSE and PSNR evaluation metrics are added in part because the standard Color-Checker Chart image (ground-truth image) can be obtained. The results of different methods can be seen in Fig. 15. The values of the chosen evaluation metrics are shown in Table 2. The values in bold represent the best results.

As shown in Figs. 15(a)–15(c), the red part decreases the most with the increase of the water depth, which is followed by the green part and then the blue part. As can be seen in Figs. 15(d)–15(i), the methods of Fu et al., He et al., and Galdran et al. cannot accurately restore the color of the underwater Color-Checker Chart images and introduce

**Table 2** Values in terms of MSE, PSNR, ENTROPY, PCQI, UCIQE, and VER.

Image	Method	MSE	PSNR	ENTROPY	PCQI	UCIQUE	VER
Fig. 15(b)	Fu et al.	4302.1	11.794	<b>7.6247</b>	<b>0.1842</b>	0.4214	<b>1.3495</b>
	He et al.	2977.1	13.393	7.0875	0.1691	0.4036	1.0585
	Galdran et al.	3211.7	13.063	7.1849	0.1671	0.4224	1.1608
	Our	<b>2905.2</b>	<b>13.499</b>	7.0478	0.1630	<b>0.4795</b>	1.1172
Fig. 15(c)	Fu et al.	3171.2	13.119	<b>7.5362</b>	<b>0.2139</b>	0.3254	<b>1.9745</b>
	He et al.	2069.2	14.973	6.8530	0.1805	0.3221	1.0149
	Galdran et al.	2363.9	14.3946	6.8955	0.1835	0.3897	1.0792
	Our	<b>1935.1</b>	<b>15.2638</b>	7.0011	0.1717	<b>0.4014</b>	1.4041

color cast (see the yellow patches). Compared with other methods, our method can recover the underwater Color-Checker Chart images taken at the depths of 5 and 15 m to relatively genuine color, though the saturation control parameter in our color cast removal algorithm is estimated using different Color-Checker Chart images taken at different depths.

In order to compute MSE and PSNR, the size and orientation of the restored Color-Checker Chart images are adjusted to match those of the standard Color-Checker Chart image. In addition, we extract the color board areas to compute MSE and PSNR values. In terms of ENTROPY, PCQI, UCIQE, and VER, the whole Color-Checker Chart image is used to compute the values of these evaluation metrics. As shown in Table 2, the lowest MSE values and highest PSNR values demonstrate that our method best restores the color of underwater Color-Checker Chart images to that of the standard Color-Checker Chart image. The best UCIQE values mean that our method can effectively balance chroma, saturation, and contrast of the enhanced Color-Checker Chart images. The highest ENTROPY, PCQI, and VER values show that the method of Fu et al. effectively improves the contrast and edge information of underwater Color-Checker Chart images.

## 5 Conclusions

In this paper, an underwater image-enhancement method, which includes a color cast removal algorithm and a visibility restoration algorithm, has been presented. The proposed color cost removal algorithm is simple yet effective. The proposed visibility restoration algorithm can minimize the information loss of enhanced underwater images based on the minimum information loss principle and the characteristics of light traveling in water. Experimental results demonstrate that our results are characterized by relatively genuine color, natural appearance, and improved visibility and contrast. In addition, our method is comparable to and even better than seven state-of-the-art methods. However, our method also shows some limitations. For example, the proposed global background estimation algorithm requires that the input underwater images have background areas. The results are

not good enough when our method processes the raw underwater images, which just have foreground areas.

## Acknowledgments

This work was supported by the National Key Basic Research Program of China (2014CB340400) and the National Natural Science Foundation of Qinghai Province of China (2015-ZJ-721). The authors thank Miao Yang, an associate professor of the Department of Electronic Engineering, HuaiHai Institute of Technology, and Arocot Sowmya, a professor of the School of Computer Science and Engineering, University of New South Wales, for providing the code of the UCIQ evaluation metric. The authors sincerely thank the editors and anonymous reviewers for their valuable comments.

## References

1. A. Yamashita, M. Fujii, and T. Kaneko, "Color registration of underwater images for underwater sensing with consideration of light attenuation," in *Proc. IEEE Int. Conf. on Robotics and Automation*, pp. 4570–4575 (2007).
2. B. L. McGlamery, "A computer model for underwater camera systems," *Proc. SPIE* **0208**, 221 (1980).
3. R. Schettini and S. Corchs, "Underwater image processing: state of the art of restoration and image enhancement methods," *EURASIP J. Adv. Signal Process.* **2010**(1), 1–14 (2010).
4. Y. Schechner and N. Karpel, "Clear underwater vision," in *Proc. IEEE Conf. on Computer Vision and Pattern Recognition*, pp. 536–543 (2004).
5. M. Ludvigsen et al., "Applications of geo-referenced underwater photo mosaics in marine biology and archaeology," *J. Oceanogr.* **20**(4), 140–149 (2007).
6. N. J. C. Strachan, "Recognition of fish species by colour and shape," *J. Image Vis. Comput.* **11**(4), 2–10 (1993).
7. L. A. Torres-Méndez and G. Dudek, "Color correction of underwater images for aquatic robot inspection," in *Proc. Fifth Int. Conf. on Energy Minimization Methods in Computer Vision and Pattern Recognition (EMMCVPR '05)*, pp. 60–73, Springer-Verlag, Berlin, Heidelberg (2005).
8. G. L. Foresti, "Visual inspection of sea bottom structures by an autonomous underwater vehicle," *IEEE Trans. Syst. Man Cybern. B* **31**(5), 691–705 (2001).
9. K. Iqbal et al., "Underwater image enhancement using an integrated color model," *IAENG Int. J. Comput. Sci.* **32**(2), 239–244 (2007).
10. K. Iqbal et al., "Enhancing the low quality images using unsupervised colour correction method," in *Proc. IEEE Int. Conf. on Systems Man and Cybernetics*, pp. 1703–1709 (2010).
11. C. Ancuti et al., "Enhancing underwater images and videos by fusion," in *Proc. IEEE Conf. on Computer Vision and Pattern Recognition*, pp. 81–88 (2012).

12. X. Fu et al., "A retinex-based enhancing approach for single underwater image," in *Proc. Int. Conf. on Image Processing*, pp. 4572–4576 (2014).
13. A. S. A. Ghani and N. A. M. Isa, "Underwater image quality enhancement through integrated color model with Rayleigh distribution," *Appl. Soft Comput.* **27**, 219–230 (2015).
14. A. S. A. Ghani and N. A. M. Isa, "Enhancement of low quality underwater image through integrated global and local contrast correction," *Appl. Soft Comput.* **37**, 332–344 (2015).
15. N. Carlevaris-Bianco, A. Mohan, and R. M. Eustice, "Initial results in underwater single image dehazing," in *Proc. IEEE Int. Conf. on Oceans*, pp. 1–8 (2010).
16. J. Chiang and Y. Chen, "Underwater image enhancement by wavelength compensation and dehazing," *IEEE Trans. Image Process.* **21**(4), 1756–1769 (2012).
17. K. He, J. Sun, and X. Tang, "Single image haze removal using dark channel prior," *IEEE Trans. Pattern Anal. Mach. Intell.* **32**(12), 2341–2353 (2011).
18. H. Wen et al., "Single underwater image enhancement with a new optical model," in *Proc. IEEE Int. Conf. on Circuits and Systems*, pp. 753–756 (2013).
19. S. Serikawa and H. Lu, "Underwater image dehazing using joint trilateral filter," *Comput. Electr. Eng.* **40**(1), 41–50 (2014).
20. A. Galdran et al., "Automatic red-channel underwater image restoration," *J. Vis. Commun. Image Represent.* **26**, 132–145 (2015).
21. X. Zhao, T. Jin, and S. Qu, "Deriving inherent optical properties from background color and underwater image enhancement," *Ocean Eng.* **94**, 163–172 (2015).
22. C. Li and J. Guo, "Underwater image enhancement by dehazing and color correction," *J. Electron. Imaging* **24**(3), 033023 (2015).
23. H. Lu et al., "Contrast enhancement for images in turbid water," *J. Opt. Soc. Am. A* **32**(5), 886–893 (2015).
24. Y. Schechner and N. Karpel, "Recovery of underwater visibility and structure by polarization analysis," *IEEE J. Oceanic Eng.* **30**(3), 570–587 (2005).
25. B. Ouyang et al., "Visualization and image enhancement for multistatic underwater laser line scan system using image-based rendering," *IEEE J. Oceanic Eng.* **38**(3), 566–580 (2013).
26. D. M. He and G. G. L. Seet, "Divergent-beam lidar imaging in turbid water," *J. Opt. Laser Eng.* **41**(1), 217–231 (2004).
27. J. Kim et al., "Optimized contrast enhancement for real-time image and video dehazing," *J. Vis. Commun. Image Represent.* **24**(3), 410–425 (2013).
28. Y. T. Peng, X. Zhao, and P. C. Cosman, "Single underwater image enhancement using depth estimation based on blurriness," in *Proc. IEEE Int. Conf. on Image Processing*, pp. 4952–4956 (2015).
29. S. Emberton, L. Chittka, and A. Cavallaro, "Hierarchical rank-based veiling light estimation for underwater dehazing," in *Proc. British Machine Vision Conf. (BMVC)*, pp. 125.1–125.12 (2015).
30. K. He, J. Sun, and X. Tang, "Guided image filtering," *IEEE Trans. Pattern Anal. Mach. Intell.* **35**(6), 1397–1409 (2013).
31. H. Gordon, "Can the Lambert-Beer law be applied to the diffuse attenuation coefficient of ocean water?," *Limnol. Oceanogr.* **34**(8), 1389–1409 (1989).
32. S. Q. Duntley, "Light in the sea," *J. Opt. Soc. Am.* **53**(2), 214–233 (1963).
33. L. S. Wang et al., "A patch-structure representation method for quality assessment of contrast changed images," *IEEE Signal Process. Lett.* **22**(12), 2387–2390 (2015).
34. M. Yang and A. Sowmya, "An underwater color image quality evaluation metric," *IEEE Trans. Image Process.* **24**(12), 6062–6071 (2015).
35. N. Hautiere et al., "Blind contrast restoration assessment by gradient rationing at visible edges," *Image Anal. Stereol.* **27**(2), 87–95 (2008).

**Chongyi Li** is pursuing his PhD at the School of Electronic Information Engineering, Tianjin University, Tianjin, China. His current research focuses on digital image processing, computer vision, and especially underwater image enhancement and restoration.

**Jichang Guo** received his BS degree from Nanjing University of Science and Technology, Jiangsu, China, in 1988 and his MS and PhD degrees in signal and information processing from the School of Electronic Information Engineering, Tianjin University, Tianjin, China, in 1993 and 2006, respectively. He is currently a full-time professor at Tianjin University. His current research interests include digital image processing, video coding, computer vision, and stereo video.

**Bo Wang** is pursuing his PhD at the School of Electronic Information Engineering, Tianjin University, Tianjin, China. His research interests include image processing, pattern recognition, computer vision, and machine learning.

**Runmin Cong** is pursuing his PhD at the School of Electronic Information Engineering, Tianjin University, Tianjin, China. His research interests include image processing, three-dimensional imaging, and computer vision.

**Yan Zhang** is pursuing his PhD at the School of Electronic Information Engineering, Tianjin University, Tianjin, China. She is a lecturer at Tianjin Chengjian University, Tianjin, China. Her research interests include digital imaging processing and intelligent information processing.

**Jian Wang** received his PhD from the Institute of Image Communication and Information Processing, Shanghai Jiaotong University, Shanghai, China, in 2006. He is currently a lecturer at the School of Electronic Information Engineering, Tianjin University, Tianjin, China. Since 2015, he has been a postdoctoral researcher at the National Ocean Technology Center, Tianjin, China. His research interests include color image processing, document image analysis, and computational photography.